Iranian (Iranica) Journal of Energy & Environment
Journal Homepage: www.ijee.net
IJEE an official peer review journal of Babol Noshirvani University of Technology, ISSN:2079-2115

Adsorption, Kinetic and Thermodynamic Study for Removal of Nickel Ions by Activated Carbon from Palm Kernel

M. Erhayem[1]*, R. Gaith[2], O. E. Otman[1], M. U. Frage[1]

[1] *Chemistry Department, Faculty of Science, Sebha University, Sebha, Libya*
[2] *Department of Chemistry, Faculty of Science, Sirte University, Sirte, Libya*

P A P E R I N F O

Paper history:
Received 09 October 2020
Accepted in revised form 30 November 2020

Keywords:
Adsorption isotherms
Adsorption kinetic
Nickel
Palm kernel
Thermodynamic

A B S T R A C T

Palm kernel (PK) was activated by chemical activation (HNO_3 at 230°C) to remove Ni(II) ions from aqueous solutions. Physicochemical properties of PK were reported. FT-IR analysis revealed changes in wave numbers and absorbance indicating Ni(II) adsorption onto activated carbon-PK surface. Energy dispersive X-ray fluorescence technique was used to determine the content of metals in activated carbon-PK and showed the metals found in activated carbon-PK were in recommended human usages. The maximum removal of Ni(II) ions was to be 49.7% at pH 4.6 and the equilibrium reached at 80 min. The removal efficiency of Ni(II) ions increased as the dosage of activated-PK increases and the optimum amount of activated carbon-PK dose was found to be 70 mg. The optimum pH was 4.6. The isotherm, kinetics and thermodynamics were studied. The Ni(II)- activated carbon-PK adsorption was found to follow the Freundlich isotherm based on correlation coefficient (R^2) values and to be physical adsorption from the mean free energy found by Dubinin-Radushkevich, which confirmed by isothermal microcalorimetry data and the heat of sorption process using Temkin Isotherm model to be 1.58 kJ/mol. The adsorption kinetic data were described well by a second order, with the kinetic constant rates in the range of 1.82-83.5 g/g.min and was not controlled by intra-particle diffusion model. The thermodynamic studies showed that the Ni(II)-ACPK adsorption process is exothermic due to the negative values of ΔH (-30.9 J/mol) and is physical nature process due to the negative values of ΔS (-14.9 J/mol). The magnitude of Ea is 15.04 kJ/mol, which is proven the physical adsorption in nature.

***doi**: 10.5829/ijee.2020.11.04.12*

INTRODUCTION

For the last decay, the level of toxic heavy metals in fresh and ground waters have been gradually increased due their release of untreated industrial efluents. Nickel is a heavy metal and has broad industrial applications such as in stainless steel for 11% total nickel processing like electroplating idustries within the ragne of 20-200 mg/l. However, the acceptable nickle in drinking water is 0.01 mg/l. The wastwaters can contain certain amout of nickel from nickel processing. High exposure to nickel has been found to be linked to cancer, sink irritation, and asthma. Therefore, nickel should be removed from these processes before discharge to the enviroment.

The removal of different heavy metals from wastewater like nickel is a big matter for the governments, environmental agencies and researchers dealing with the production of water sources and ecosystems for more than a decay [1]. Among to several chemical and physical techniques have been used in the big scale to remove these heavy metals from wastewater, such as conventional technologies, separation methods, etc. Adsorption has been found to be one of the simplest, low cost and high effciency techniques used for purification of waters in industries [2, 3]. This techinge uses to immobilize ions from liquid phase onto solid phase by using diffenent materials, such as activated carbon [2]. Almost, all carbon-rich materials from plants may be used to remove these heavy metals from an aqueous solution. Activated carbon form after either physical or chemical carbonization processes are found to be more useful products like activated carbon if carefully controlled processes of dehydration, carbonization, and physical and chemical activation [4, 5]. These agricultural wastes have been increasingly in demand for activated carbon in industrial processes due to their ability to absorb any organic solvent at low temperature and release it at high temperature [6]. The adsorption of heavy metals onto waste agricultural materials could be related to their lignin, cellulose and

*Corresponding Author E-mail: moh.erhayem@sebhau.edu.ly (M. Erhayem)

Please cite this article as: M. Erhayem, R. Gaith, O. E. Otman, M. U. Frage, 2020. Adsorption, Kinetic and Thermodynamic Study for Removal of Nickel Ions by Activated Carbon from Palm Kernel, Iranian (Iranica) Journal of Energy and Environment, 11(4): 339-350.

hemicellulose with carboxylic, hydroxyl, sulphate, phosphate and amino groups that can bind to heavy metal ions [7].

Many studies have reported on the development of these activated carbon from low cost and readily available natural materials [7, 8]. One of widespread heavy metals use in many industrial applications is nickel (Ni) ions with small quantities (0.1-0.6 ppm) in natural ecosystems [9]. The non-degradable Ni metals present in the Eco environments from the large scale industrialization such as mining, electroplating, tanning, metallurgical operation and manufacturing leads to serious problems on aquatic life, animal, plant life and human health even at low concentrations [7].

The removal of heavy metals is a matter of great interest for researchers and environmental agencies because of their toxicity, reactivity and mobility in soil and waters [10]. The main objectives of this study were: to offer effective and economical adsorptive materials and to investigate its ability for the adsorption of Ni(II) ions from aqueos solution and to study the isotherm, kinetic and thermodynamic of Ni- activated carbon-PK adsorption processes .

MATERIALS AND METHODS

All chemicals used in this research were purchased from different companies, Scharlau, BDH chemicals Ltd and Surechem products Ltd, and were used without further purification. The Ni(II) stock solution was prepared by dissolving an accurately amount of nickel chloride ($NiCl_2.6H_2O$) from BDH chemicals Ltd–in deionized water. The desired concentrations of Ni(II) were prepared by diluting the Ni (1000 mg/l) stock solution with deionized water. Nitric acid was used for the activation. pH of the solution was adjusted with Hydrochloric acid and sodium hydroxide. from Scharlau.

pH meter and cnductivity meter were used for pH and conductivity measurements. These instruments were supplied from Thermo, Orion 4 star and cnductivity meter from Philips, PW-9527.

Analyzer EA-1112 was used from thermo for CHNS analysis. Oxygen was used to combust activated carbon-PK and helium was used as carrier gas. The furance was set to 950°C at the intial and geses were flowed. A few mg of PACK was put on the alumnium foile. Thermal conductivity detector was used for analyze CHNS.

Atomic absorption spectrophotometer from Thermo AA spectrometer S- series was used for Ni conccentration before and after andrption processes.

In this research, Fourier transform infrared (FT-IR) and spectrometer were used for characherization of the surface of PK and to identify chemical functional groups presnt on the surface of PK. Samples were scaned with an Burker instrument and resolution 2 cm^{-1} over spectral range extending from 4000 to 400 cm^{-1}.

Surface area of activated carbon-PK was determined by BET method from nitrogen adsorption resulting isotherm at 77 K in an automatic analyzer (Micromeritics 2020 ASAP apparatus) after pre-treatment for 3 h at 473 K under vacuum.

Energy dispersive X-ray fluorescence, EDXRF, NEX QC+QuantEZ from Rigaku was used for the determination of elements present in activated carbon-PK. All measurements were carried out under helium and the tube voltage (kV) was High-Z 50.0, Mid-Z 30.0 and Low-Z Open 6.5. FP method was used for analysis. 4g was put it onto the EDXRF container. XRF thin film (TF-240, polypropylene) from premier lab supply was used.

Differential heat flow reaction calorimeter (TITRYS, from Setaram) equipped with a stirring system used for heat measurment.

Adsorbent collection and preparation was carried out according to previous method developed with slight modifications [11]. The PK as low-value or zero cost agricultural waste production especially in Libya was collected from Sirte reagon, north part of Libya. The collected PK samples were frist washed with distilled water for several times in order to remove the dirt, dust and fine. Then, dried in an oven at 378 K for 24 h and later grounded to obtain a powder form and sieved to a 1.0 mm to 0.5 mm.

The chemical activation process for PK was carried out by following method with slight modifications [12]. 100 ml of HNO_3 (65%, w/w) was mixed with 20 g of PK with ratio 1:5 (raw PK:HNO_3). The suspension of PK-HNO_3 was allowed to soak at 383 K for 3 hours and then left to cool for overnight at room temperature in closed container. The activated carbon palm kernel (ACPK) was washed with distilled water until the pH remained constant. Then, ACPK was dried at 378 K for 24 hours. Finally, ACPK samples were heated at 473 K, crushed, sieved at 125 µm and stored in desiccator.

The effect of time at which the equilibrium of Ni(II)-ACPK adsorption was investigated. 0.1 to 1.0 g of ACPK was added to 150 ml of 20.0 mg/l Ni(II) solution at 298 K. The suspension was placed on a stirring plate for 120 min. During the experimental time period, 5 ml aliquots of Ni(II)-ACPK suspensions were filtered at various time intervals (0 to 120 min). The percentage removal of Ni(II) was investigated by adding 50 mg of ACPK to different Ni(II) concentrations from 5 to 25 mg/l at a pH of 4.6, agitation speed 200 rpm, contact time 80 min and T=298, 308 and 318 K. The effect of ACPK dose on Ni(II)-ACPK adsorption was investigated by adding 0.1 to 1.0 g of ACPK to 20 mg/l Ni(II) ions, pH of 4.6, contact time 80 min and T=298, 308 and 318 K. In order to evaluate the effect of initial pH on Ni(II)-ACPK adsorption from aqueous solution, 50 mg of ACPK was added to 150 ml of 20 mg/l Ni(II) at different pH values

(3.0 to 7.0), agitation speed 200 rpm, contact time 80 min and T=298, 308 and 318 K. During the experimental time period, 5 ml aliquots of Ni(II)-ACPK suspensions were taken and filtered with 0.45µm filter paper. The filtrate was analyzed for Ni(II) concentration by AAS. All the experiments were carried out triplicate runs and the average values were taken. The amount of Ni(II) ions adsorbed onto ACPK surface per unit of mass (q_{max}, mg/g) was evaluated by the following equation:

$$q_{max} = \frac{C_o - C_e}{W} \times V \quad (1)$$

where: initial Ni(II) concentration (C_o, mg/l); final Ni(II) concentration at equilibrium (C_e, mg/l), volume of Ni(II) solution (V, ml); mass of ACPK sample (W, mg). The percent sorption of Ni(II) was also evaluated by the following equation:

$$\%\text{Removal} = \frac{C_o - C_e}{C_o} \times 100 \quad (2)$$

In order to measure the heats of Ni(II)-ACPK adsorption, a calorimeter equipped with a stirring system and a system for the introduction of liquids (a programmable syringe pump PHD 2000, from Harvard Apparatus, linked to the calorimeter by capillary tubes), in aqueous phase was used. Successive pulse injections of 20 mg/l solution of Ni(II) ions in deionised water were sent to the sample maintained at 303 K at 2 hours time intervals. Water and the aqueous solution of Ni(II) used in this study were previously purged with flowing nitrogen to avoid forming of air bubbles in the capillary tubes. A preheating furnace was used to allow the injection of the probe solution at the same temperature of 303 K. The reference and measurement cells contained water (1.5 ml) and water with a weighted amount of the solid sample (cal. 100 mg), respectively. The samples were activated in situ by outgassing the powders at 323 K for 2 hours and then transferred into the calorimeter cell. The evolved heat from the adsorption processes was obtained by using the integration of the area under the calorimeter signal for each dose.

RESULTS AND DISCUSSION

The proximate composition of ACPK was carried according to previous methods [13, 14]. The ACPK characteristics, which are essential to understand the adsorptive behavior, are presented in Table 1.

The moisture content was found to be high, which might be due to its plant origin of PK. Ash content was high which might be related to acid and water wash might not have been able to reduce leachable ash or the presence of substantial amounts of water-soluble minerals remained in the ACPK sample. Conductivity and salinity of ACPK were used to indicate the quality of activated carbon and found to be slightly high comparing to those of other studies which might be due to the presence of soluble minerals in surface of ACPK after carbonization process [13]. The bulk density is important parameter for biosorption application because the higher bulk density is better the filterability of activated carbon. The bulk density of ACPK was found to be generally higher than lower limit of 0.25 g/cm^3 for granular activated carbon. The pH of ACPK was acidic 4.8, which this might be due to the acid wash was incomplete or the nature of PK. It was found that the suspension pH affects the rate of activated carbon adsorption, which is more effective at low pH than high pH [14]. Further, surface area is an important parameter to achieve the adsorption behavior of the biocarbon. It was found that the surface area of ACPK was 1.13 m^2/g, using Brunauer, Emmet, and Teller (BET) method. These results are indicated the biocarbon with a good activity for adsorption with one exception.

The EDXRF results of the ACPK samples for contained oxide elements are shown in Figure 1 and additional data are listed in Table 2. The EDXRF results of the ACPK samples for contained elements as shown in Figure 1 and listed in Table 3. These results indicated that the ACPK can be used for water purification process.

Figure 2 shows the FT-IR spectrum of ACPK-Ni(II). 50 mg of ACPK was added to 150 ml of 20 mg/l Ni(II) at a pH of 4.6, agitation speed 200 rpm, contact time 80 min (time study) and T= 298 K. The spectrum revealed the presence of the following groups: a peak at 3361.05 cm^{-1} assigned with –OH group belongs to cellulose or lignin [15]. After addition of Ni(II) ions, this peak was shifted from 3361.05 to 3363.44 cm^{-1} and the percentage of peak transmittance was increased from 92.8 to 98.2%, which was probably due to complexation of Ni(II) with ionized –OH group of hydroxyl group and bonded -OH bands of carboxylic acids in the inter- and intra-molecular hydrogen bonding of polymeric compound [15]. Furthermore, carbonyl group (>C=O stretch) peak at 1741.85 cm^{-1} and the peak appeared at 1611.97 cm^{-1} assigned with N-H bend stretching from amide groups were observed and a change of these peaks was also

TABLE 1. Physico-chemical characteristics of ACPK

Physico-chemical properties	Value	Physico-chemical properties	Value
Moisture content (%)	7.28	Matter soluble in water	0.190
Ash content (%)	5.80	N (%)	6.94
Bulk density (g/cm^3)	0.35	C (%)	24.5
pH	4.80	H (%)	2.65
Conductivity (µS/cm)	285	S (%)	8.13
Salinity (mg/l)	163	net heat value (kcal/kg)	3125
S_{BET} (m^2/g)	1.13	gross heat value (kcal/kg)	2989

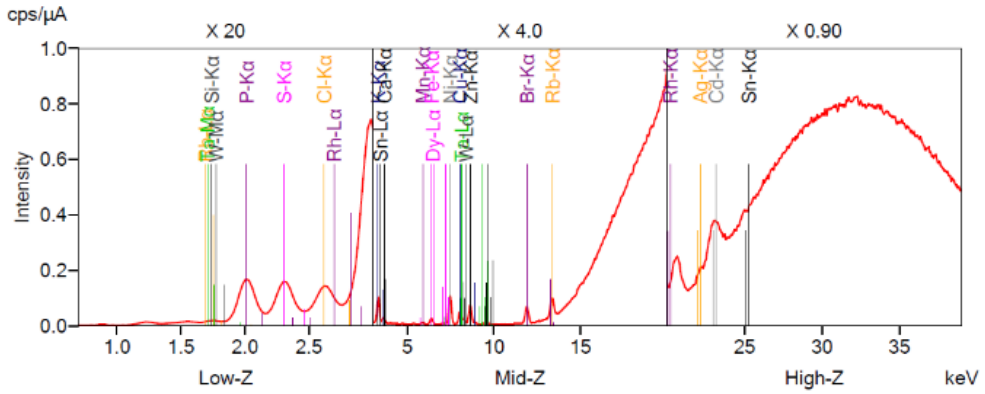

Figure 1. EDXRF spectrum of ACPK for oxide element analysis method

noted after the addition of Ni(II). The peak at 1036.88 cm^{-1} assigned to the surface -C-O bond stretching of phenolic groups. Therefore, FT-IR studied revealed that several functional groups present in ACPK are likely to bind the Ni(II) ions and to suggest considerable cation exchange capacity to adsorbent surface [16].

Figure 3 shows the effect of contact time on the removal of Ni(II) onto the surface of ACPK. 0.1 to 1.0 g of ACPK was added to 150 ml of 20 mg/l Ni(II) at a pH of 4.6, agitation speed 200 rpm and T=298K. The ACPK-Ni(II) adsorption was shown a similar trend with respect to time, but the extent of removal was differed. Generally, the trend was a rapid increase in Ni(II) ions removal after addition of ACPK, followed by leveling off towards the end of the experiment at certain time. The AAS data clearly shows that no significant additional adsorption of Ni(II) onto ACPK surface ccurred after 40 min. Thus, 80 min was chosen as the time the equilibrium of ACPK-Ni(II) adsorption was attained.

Figure 4 shows the effect of initial Ni(II) concentration on the percentage removal of Ni(II) by ACPK. 50 mg of ACPK was added to 150 ml of different concentrations of Ni(II) (5 to 25 mg/l) at a pH of 4.6, agitation speed at 200 rpm, contact time at 80 min and T at 298 K. It was found that the percentage removal of Ni(II) by ACPK was decreased with increasing in

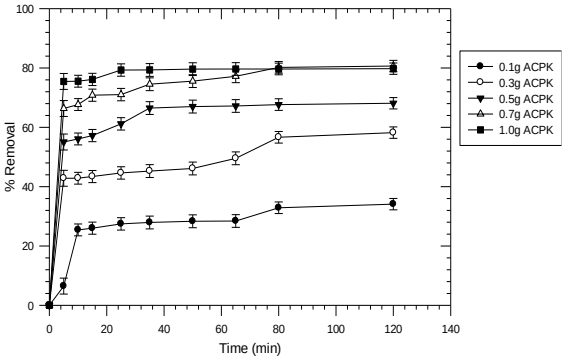

Figure 3. Effect of contact time on the removal of Ni(II) by ACPK. 0.1 to 1.0 g of ACPK was added to 150 of 20 mg/l Ni(II) at a pH of 4.6, agitation speed 200 rpm and T=298K

Figure 2. FT-IR spectrum of ACPK-Ni(II). 50 mg of ACPK was added to 150 ml of 20 mg/l Ni(II) at a pH of 4.6, agitation speed 200 rpm, contact time 80 min (time study) and T=298K

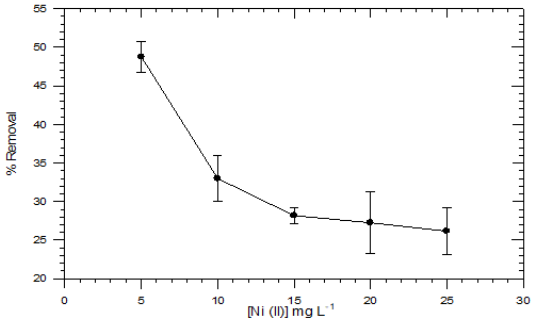

Figure 4. Effect of initial Ni(II) concentration on the percentage removal of Ni(II) by ACPK. 50mg of ACPK was added to 150 ml of different concentrations of Ni(II) (5 to 25 mg/l) at a pH of 4.6, agitation speed 200 rpm, contact time 80 min and T=298K

TABLE 2. The EDXRF results of ACPK for oxide metals

No.	Component	Result	Unit	Stat.Err.	LLD	LLQ
1	K_2O	63.5	mass%	0.65	0.907	2.72
2	P_2O_5	28.2	mass%	0.0522	0.0465	0.14
3	CaO	19.1	mass%	0.793	1.73	5.2
4	SO_3	15.4	mass%	0.0312	0.0384	0.115
5	NiO	4.03	mass%	0.0517	0.0118	0.0353
6	SiO_2	2.96	mass%	0.0356	0.0833	0.25
7	Fe_2O_3	2.31	mass%	0.0616	0.0727	0.218
8	MnO	1.75	mass%	0.0643	0.0385	0.116
9	ZnO	1.65	mass%	0.0247	0.0079	0.0236
10	CuO	1.37	mass%	0.0267	0.0282	0.0846
11	Dy_2O_3	0.934	mass%	0.0999	0.279	0.837
12	Ta_2O_5	0.423	mass%	0.0568	0.17	0.509
13	CdO	0.36	mass%	0.0057	0.014	0.0419
14	WO_3	0.336	mass%	0.0373	0.0947	0.284
15	Rh_2O_3	0.297	mass%	0.0052	0.0107	0.0322
16	Rb_2O	0.294	mass%	0.0058	0.0112	0.0335
17	Ag_2O	0.0575	mass%	0.0038	0.0105	0.0315
18	SnO_2	<0.0001	mass%	0.007	0.0211	0.0633

TABLE 3. The EDXRF results of ACPK for elements

No.	Component	Result	Unit	Stat.Err.	LLD	LLQ
1	K	52.7	mass%	0.54	0.753	2.26
2	Ca	13.6	mass%	0.567	1.24	3.72
3	P	12.3	mass%	0.0228	0.0203	0.0609
4	S	6.17	mass%	0.0125	0.0154	0.0462
5	Ni	3.16	mass%	0.0406	0.0093	0.0278
6	Cl	2.57	mass%	0.007	0.0127	0.0382
7	Fe	1.62	mass%	0.0431	0.0508	0.153
8	Si	1.38	mass%	0.0166	0.0389	0.117
9	Mn	1.35	mass%	0.0498	0.0298	0.0895
10	Zn	1.32	mass%	0.0199	0.0063	0.0189
11	Cu	1.09	mass%	0.0213	0.0225	0.0676
12	Dy	0.814	mass%	0.0871	0.243	0.729
13	Br	0.398	mass%	0.0059	0.004	0.0119
14	Ta	0.346	mass%	0.0466	0.139	0.417
15	Cd	0.315	mass%	0.005	0.0122	0.0367
16	Rb	0.269	mass%	0.0053	0.0102	0.0306
17	W	0.267	mass%	0.0295	0.0751	0.225
18	Rh	0.241	mass%	0.0042	0.0087	0.0261
19	Ag	0.0535	mass%	0.0035	0.0098	0.0293
20	Sn	<0.0001	mass%	0.0055	0.0166	0.0498
21	O	<0.0001	mass%			

initial Ni(II) concentrations. This may due to the ratio of available ACPK surface active sites to Ni(II) at low concentration is high and decreased with increasing Ni(II) concentration. Therefore, lower concentrations of Ni(II) were used to study the kinetic and isotherm models.

Figure 5 shows the effect of adsorbent dose on the removal of Ni(II) by ACPK. Different amounts of ACPK (0.1 to 1.0 g) were added to 150 ml of 20 mg/l Ni(II) at a pH of 4.6, agitation speed 200 rpm, contact time 80 min and T=298K. As expected, the removal efficiency of ACPK was significantly increased with increasing ACPK doses from 0.1 to 1.0 g. This may be due to availability of more surface area with the higher dose of ACPK in solution [17]. The maximum removal of Ni(II) by ACPK is 77.6% for adsorbent of 70mg per 150 ml of Ni(II) solution, while no significant additional Ni(II) adsorption onto ACPK occurred after 70mg of ACPK. This might due to aggregation/agglomeration of adsorbent particles at higher concentrations leading to decrease in the total ACPK surface active sites for adsorption or over crowding the adsorbent particles [18].

Figure 6 shows the effect of pH on the removal of Ni(II) ions by the surface of ACPK. 50 mg of ACPK was added to 150 ml of 20 mg/l Ni(II) at different pH, agitation speed 200 rpm, contact time 80 min and T=298K. The removal efficiency increases with increasing in solution pH from 3 to 4.6 and then decreases with increasing in solution pH. This could be due to the concentration of protons which are released from active sites of ACPK is high at low pH, so the Ni(II) ions and the protons compete for binding sites of the ACPK surface which decrease with increasing pH, namely electrostatic interaction mechanism. At high pH, the degree of protonation of ACPK functional groups decreased gradually and therefore the efficiency of Ni(II) removal decreased as well due to neutralization of the ACPK surface. The optimal Ni(II) removal efficiency was at pH 4.6 due to the negative charge density on the ACPK surface. Also, pH affects the solubility of Ni(II) in solution and ions on the functional groups of ACPK. Therefore, the uptake of Ni(II) by ACPK is pH-dependent. A similar result was obtained when other adsorbents were used [19-21].

Figure 7 shows equilibrium concentration of Ni(II) ions as function of solution temperature. 0.1 g of ACPK was added to 150 ml of 5 to 25 mg/l Ni(II) at a pH of 4.6, agitation speed at 200 rpm and T at 298, 308 and 318 K. It can be seen that the percentage removal of Ni(II) on ACPK decreases as the temperature increases. This result confirms that the adsorption process is exothermic. The decrease in Ni(II) adsorption on ACPK surface as temperature increases may be due to the relative increase in escaping tendency of Ni(II) ions from solid phase to solution phase. Also, this could be due to the weakness of adsorptive forces between Ni(II) and active sites on ACPK [22]. Therefore, the increasing in solution temperature may be used to recover the active sites on ACPK.

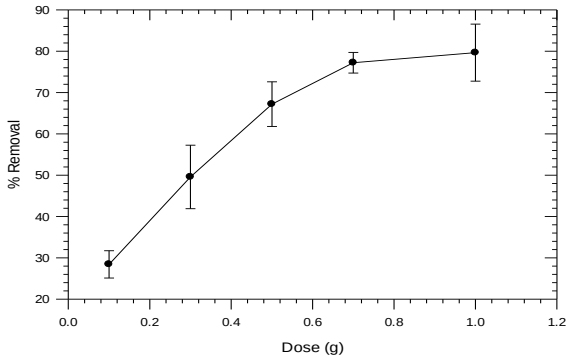

Figure 5. Effect of adsorbent dose on the removal of Ni(II) by ACPK. Different amounts of ACPK (0.1 to 1.0 g) were added to 150 ml of 20 mg/l Ni(II) at a pH of 4.6, agitation speed 200 rpm, contact time 80 min and T=298K

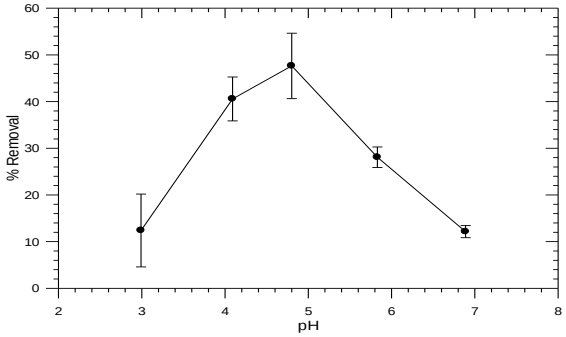

Figure 6. Effect of pH on the removal of Ni(II) by ACPK. 70mg of ACPK was added to 150 ml of 20 mg/l Ni(II) at different pH, agitation speed 200 rpm, contact time 80 min and T=298K

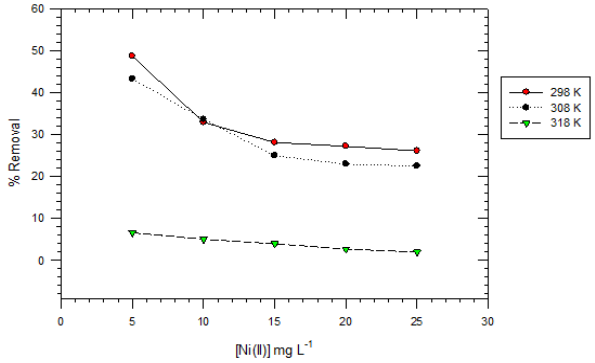

Figure 7. Equilibrium concentration of Ni(II) ions as function of solution temperature. 0.1 g of ACPK was added to 150 dm^3 of 5 to 25 mg/l Ni(II) at a pH of 4.6, agitation speed 200 rpm and T=298, 308 and 318K

Adsorption isotherms

The Freundlich isotherm model is useful to identify sorption phenomena of ACPK-Ni(II) adsorption process and can be determined by following equation:

$$q_e = K_F C_e^{1/n} \quad (3)$$

where: adsorption equilibrium constant (K_F, mg/g $(l/g)^{1/n}$); amount of Ni(II) per unit mass of adsorbate (q_e, mg/g); equilibrium concentration (C_e, mg/l) [23]. A straight line was obtained by plotting q_e versus C_e and the results are listed in Table 4. Based on Freundlich assumptions, a smaller value of 1/n indicates that weak adsorptive forces are effective on the ACPK surface at all temperatures. Therefore, the process was favorable sorption even at higher Ni(II) concentrations [16, 17]. Also, the decrease in K_F and 1/n values with increasing temperature indicates that the adsorption process is exothermic [18].

Langmuir model assumes the monolayer sorption occupied onto the surface containing a finite number of identical sorption site and can be described by the following equation:

$$q_e = \frac{bC_e q_m}{1+bC_e} \quad (4)$$

where: the maximum Ni(II) ions uptake per unit mass of ACPK (q_m, mg/g); Langmuir equilibrium constant (b, L/g). A plot of C_e/q_e versus C_e yields a straight line with its slop of $1/q_e$ and intercept of $1/q_e b$ and results are listed in Table 2**.** The experimental values of *b* were slightly increased with the increase of temperatures, indicating that a smaller heat of adsorption was liberated with increasing temperature. The q_e value was decreased with increasing solution temperature from 298 to 318K, indicating the weak adsorption interactions between Ni(II) and ACPK at high temperature, which support the physic-sorption. This may be due to the destruction of the active sites on ACPK matrix with increasing solution temperature [16]. This confirms that the ACPK-Ni(II) adsorption process is exothermic.

Also, the Langmuir model can be used to evaluate the constant separation factor, R_L, as expressed by the following equation:

$$R_L = \frac{1}{1+bC_o} \quad (5)$$

The value of R_L indicates the isotherm shape to be unfavorable (R_L>1), favorable (0<R_L<1) and irreversible (R_L=1) [19]. The magnitude of R_L was found to be less than unity showing that ACPK-Ni(II) adsorption was most favorable under different temperature studied under these conditions using Langmuir isotherm.

The D-R equation has the following form:

$$q_e = q_{max}\, e^{-\beta\varepsilon^2} \quad (6)$$

where q_{max}: D-R monolayer capacity (mg/g); β is a constant related to sorption energy and ε is Polanyi potential. The DKR parameters are calculated from the slop of the plot of ln q_e versus ε gives β (mol^2/J^2) and intercept gives q_m (mg/g). The β means free energy (E) of sorption per molecule of the sorbate when it is transferred to the surface of the solid from infinity in the solution:

$$E = \frac{1}{\sqrt{2\beta}} \quad (7)$$

The magnitude of E is used to estimate the adsorption mechanism [15]. The value of E is <8 (1.58 kJ/mol) that reveals the sorption process follows physical sorption, TABLE 4. This may be due to the surface area of ACPK was relatively low (S_{BET}=1.13 m^2/g) as comparing to other studies. Therefore, the attraction between the Ni(II) and PK surface was a weak Van der Waals attraction due ACPK-Ni(II) physisorption.

The linear form of Temkin isotherm taking into an account of adsorbent-adsorbate interactions is represented by the following equation:

$$q_e = \frac{RT}{b}\ln A + \frac{RT}{b}\ln C_o \quad (8)$$

where: $B = \frac{RT}{b}$ constant related to heat of sorption (J/mol) obtained From the Temkin plot (q_e versus lnC_e) and listed in TABLE 4; A is Temkin isotherm equilibrium binding constant (l/g); b is Temkin isotherm constant; R is universal gas constant (8.314 J/mol/K) at different T=298, 308 and 318 K [21]. The heat of sorption, B, is lower than 8 kJ/mol, which indicating a physical adsorption process and decreased with increasing temperature suggesting the adsorption process is exothermic [12]**.**

From R^2 values given in Table 4, it can be clearly seen that the Freundlich model yields a better fit than other isotherm models used in this study. This trend probably due to high surface area, multilayer of Ni(II) adsorption onto ACPK surface and the adsorption on a surface was not containing a finite number of identical sites which is heterogenic surface and the boundary layer thickness is also increased. Also, based on R^2, it was noted that the adsorption process was followed Freundlich model at low temperature, while it was followed Langmuir model.

Figure 8 shows the results from microcalorimetric experiment for the adsorption of Ni(II) onto ACPK surface. Each pulse injection of dosed amount of 2mg/l Ni(II) in deionised water, 303 K. The heats of ACPK-Ni(II) interactions were very low nearly base line of calorimeter indicating that the Ni(II) adsorption onto ACPK surface was low. This is confirmed that the ACPK-Ni(II) adsorption was physical adsorption, which is consistent with the result obtained from Temkin isotherm.

Figure 9 shows the plots of (A) first-order, (B) second-order, (C) Elovich and (D) intra-particle diffusion and (E) Boyd model for ACPK-Ni(II) adsorption. Different ACPK doses (0.1, 0.3, 0.5, 0.7 and 1.0 g) was

TABLE 4. Freundlich, Langmuir, D-R and Temkin constants 50mg of ACPK was added to 25 ml of 5 to 25 mg/l of Ni(II) at a pH of 4.6, agitation speed 200 rpm, contact time 80 min and T=298, 308 and 318k

T (K)	Freundlich Constants			Langmuir Constants			
	K_F mg/g(L/g)$^{1/n}$	1/n	R^2	$q_{e.exp}$ mg/g	*b* L/g	R_L	R^2
298	0.783	0.491	0.9924	28.5	0.097	0.802-0.352	0.8543
308	0.584	0.463	0.9717	22.2	0.122	0.744-0.298	0.9201
318	0.047	0.406	0.8850	2.53	0.142	0.602-0.225	0.9234
T (K)	D-R constants				Temkin constants			
	q_m mg/g	ß X10^{-7}	*E* kJ/mol	R^2	B J/mg	A L/g	B J/mol	R^2
298	48.4	2.00	1.58	0.7756	0.419	1.07	5.91	0.8763
308	49.5	2.00		0.8835	0.523	1.19	4.89	0.9196
318	12.1	3.00		0.9192	4.53	1.25	0.584	0.8725

added to 150 ml of 20 mg/l Ni(II) at a pH of 7.0, agitation speed 200 rpm and T=298 K. The sorption kinetics can be described by a first-order equation:

$$\ln(q_e - q_t) = \ln q_e - k_1 t \quad (9)$$

where: k_1 is the adsorption rate (min^{-1}) and q_e (at equilibrium) and q_t (at time t) are the amount of Ni(II) adsorbed onto ACPK surface (mg/g) at time t [20]. A plot of $\ln(q_e - q_t)$ versus t gives a straight line of slop and intercept as shown in Figure 9A and the results are summarized in Table 5.

The experimental data are not well fitted for pseudo-first-order equation. This was due to the correlation coefficients (R^2) were low. Also, the large differences between $q_{e.exp}$ and $q_{e.cal}$ values were observed.

The mechanisms of the ACPK-Ni(II) adsorption was tested by pseudo second-order model:

$$\frac{t}{q_t} = \frac{1}{k_2 q_2^2} + \frac{t}{q_2} t \quad (10)$$

where: k_2 is the adsorption rate constant (g/mg.min). The plot of t/q_t versus t gives q_e=1/slop and k_2=slop^2/intercept [20]. Figure 9B shows the linearized pseudo-second order kinetic plot and the parameters were listed in Table 5. It can be seen from Table 5 that the R^2 values for all different ACPK doses are extremely high coefficients (upto 1.000). In addition, the $q_{e.cal}$ values agree with the experimental $q_{e.exp}$ from Langmuir isotherm. The values of k_2 increase with increasing ACPK concentrations. This may due to the increase in the surface active sites at high ACPK concentrations.

The mechanism of ACPK-Ni(II) adsorption was tested by Elovich model:

$$q_t = \frac{1}{\beta}\ln(\alpha\beta) + \frac{1}{\beta}\ln(t) \quad (11)$$

where: α is the initial adsorption rate (mg/g.min) and β is the adsorption constant (g/mg). Figure 9C shows the plots of q_t versus ln(t) give a linear relationship with a slope ($1/\beta$) and intercept ($1/\beta$)ln($\alpha\beta$) and the parameters were summarized in Table 5. However, the correlation coefficients for Elovich model obtained at all the studies ACPK doses were low, suggesting that the adsorption process is not an acceptable for Elovich model system.

The Weber and Morris intra-particle diffusion model was used to analyze the experimental kinetic results.

$$q_t = K_{ip} t^{0.5} + C \quad (12)$$

where: K_{ip}: the intra-particle diffusion rate constant and C: the intercept which reflects the boundary layer effect. The intra-particle parameters were determined by a plot of q_t versus $t^{0.5}$, shown in Figure 9D and summarized in Table 5. The K_{ip} values were decreased with increasing ACPK dosage. It is clears from Figure d that the linear plots at each ACPK concentration did not pass through the origin. This may due to the difference in the rate of

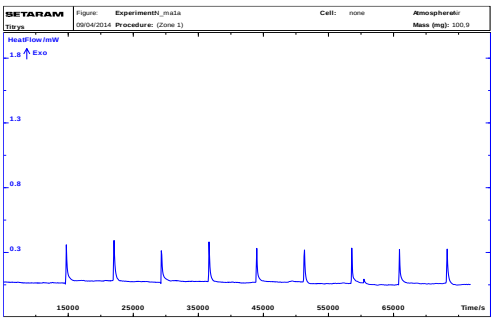

Figure 8. Typical microcalorimetric experiment for the adsorption of Ni(II) on ACPK. Each pulse injection of dosed amount of 2mg/L Ni(II) in deionised water, 303 K

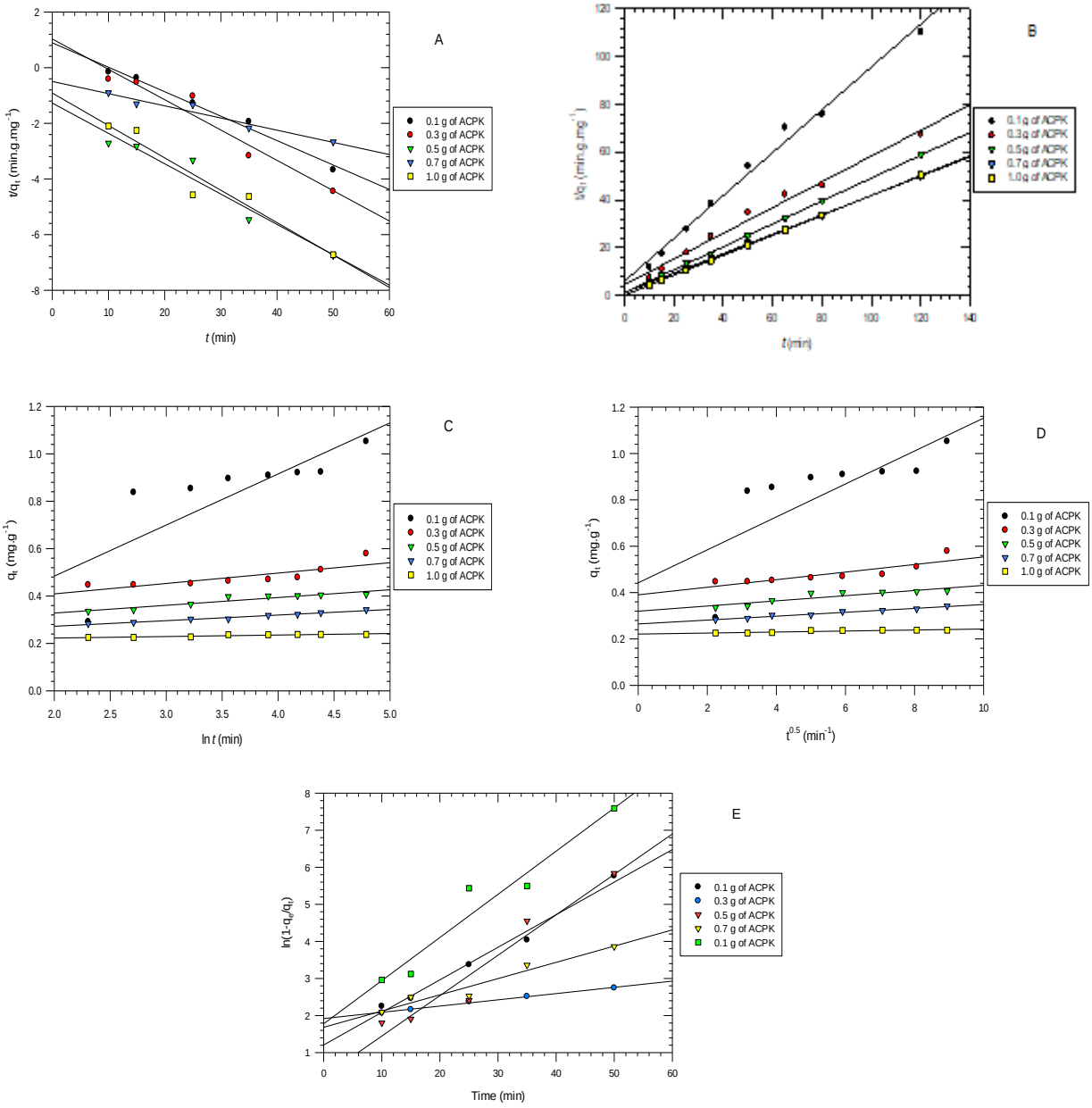

Figure 9. Plots of (A) first-order, (B) second-order (C) Elovich, (D) intra-particle diffusion and (E) Boyd model for ACPK-Ni(II) adsorption . Different ACPK doses (0.1, 0.3, 0.5, 0.7 and 1.0 g) was added to 150 ml of 20 mg/l Ni(II) at a pH of 7.0, agitation speed 200 rpm and T=298 K

mass transfer in the initial and equilibrium steps of the sorption [22]. Therefore, the intra-particle diffusion Model was not the only rate-limiting step for adsorption process of ACPK-Ni(II).

The experimental data were tested by Boyd model to determine the actual process involved in the Ni(II)-ACPK adsorption using Equation (13).

$$\log(q_m - q_t) = \log q_m - \left(\frac{R}{2.303}\right) t \qquad (13)$$

The Boyd plots as shown in Figure 9E was not linear with high correlation coefficients (R^2>0.8496), indicate that the film diffusion mainly governs the Ni(II) adsorption onto ACPK.

The Arrhenius equation is used to evaluate the activation energy (E_a, kJ/mol) by the following expression:

$$b = A\, exp^{(-E_a/RT)} \qquad (14)$$

TABLE 5. Parameters of First-order and Second-order Kinetics for Sorption of Ni(II) onto ACPK Different ACPK doses (0.1 to 1.0 g) was added to 150 ml of 20 mg/l Ni(II) at a pH of 4.6, agitation speed 200 rpm and T=298K

First order					Second order			Elovich			Intra-particle diffusion		
Dose	$q_{e\ exp}$	$q_{e\ cal}$	$k_1\times10^{-2}$	R^2	$q_{e\ cal}$	$k_2\times10^{-2}$	R^2	B	A	R^2	$K_{ip}\times10^{-2}$	C	R^2
g	mg/g	mg/g	min^{-1}		mg/g	g/mg/min					mg/g/min	mg/g	
0.1	8.16	2.45	8.79	0.9852	10.1	1.28	0.9876	1.06	514	0.8070	3.16	0.725	0.8828
0.3	4.43	0.75	1.69	0.9927	3.72	2.15	0.9650	1.69	71.1	0.7717	2.03	0.365	0.8720
0.5	3.79	2.81	1.09	0.944	3.96	8.86	0.9997	3.05	978	0.8880	0.99	0.316	0.7789
0.7	3.07	0.612	4.38	0.9477	3.37	8.45	0.9992	4.39	7192	0.9593	0.73	0.271	0.9453
1.0	2.27	2.49	11.6	0.9426	2.29	83.5	1.000	18.8	2.23E+16	0.7585	0.15	0.225	0.6142

TABLE 6. Thermodynamic parameters of Ni(II) adsorption on ACPK

T	*B*	ΔG^o	ΔH^o	ΔS^o	*Ea*
K	l/mg	kJ/mol	J/mol	J/mol	kJ/mol
298	0.0967	5.79			
308	0.122	5.39	-30.9	-14.9	15.04
318	0.142	5.17			

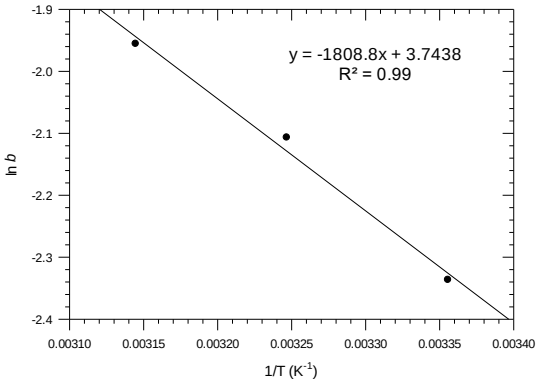

Figure 10. Arrhenius plot for adsorption of Ni(II) onto ACPK

where: A is the frequency factor. The *E*a were calculated from the plot of ln *b* versus 1/T (K^{-1}) which the slope is -*Ea*/R obtained from Figure 10. The obtained *Ea* from slope was 15.04 kJ/mol. The magnitude of *Ea* value lies in the range of 0-40 J/mol for physical sorption process [22]. This confirms that the ACPK-Ni(II) adsorption is physisorption.

The adsorption thermodynamic parameters were calculated from the Equations (15) and (16):

$$\Delta G^o = -RTlnb \quad (15)$$

$$lnb = \frac{-\Delta H^o}{RT} + \frac{\Delta S^o}{R} \quad (16)$$

where: $\Delta G^o$is a standard free energy, $\Delta S^o$is entropy, $\Delta H^o$is enthalpy, b is the Langmuir equilibrium constants and R is gas constant (8.314 J/mol/K) [19]. Van't Hoff plots (ln$b$ versus 1/T) of ACPK-Ni(II) adsorption at different initial concentrations of Ni(II) give slope ($-\Delta H^o/R$) and intercept (ΔS^o/R), while $\Delta G^o$is calculated from Equation (15) and listed in Table 6.

A negative value of ΔH^o indicates that the adsorption process takes place by an exothermic process and the magnitude value of ΔH^o (-0.0309 J/mol) was less than 2.1 J/mol and the negative values of both $\Delta H^o$and ΔS^o suggesting the physisorption of Ni(II) onto ACPK in nature and involving weak forces of attraction [23]. This result confirms the previous result which was obtained in DKR, Temkin isotherms and calorimetry data. The positive value of ΔG^osuggests the non-spontaneous nature of adsorption ACPK-Ni(II). The decrease in ΔG^ovalue with increasing in temperature indicates that the reaction is more favorable at high temperature.

CONCLUSION

The finding in this study revealed that palm kernel, which is an agricultural wastes material, can be applied in water treatment systems to remove Ni(II) ions from aqueous solutions. The effect of several parameters such as; pH, initial concentration ,contact time and dose was investigated. Results show that the study ACPK has a good adsorption capacity for nickel .The best condition for the removal of nickel was observed at pH 4.6,concentration 20 mg/l, dose 70mg with in 80 min. FT-IR analysis indicated the presence on ACPK surface of hydroxyl and carboxyl groups which reduced after the addition of Ni(II). The equilibrium was the best described by Freundlich isotherm based on correlation coefficient, while the kinetic of the process was the best described by using second order at different ACPK doses indicating heterogenic multilayer adsorption and followed by Langmuir, Temkin and D-R isotherms. From DKR and calorimetry results, the sorption energies were 1.58 kJ/mol and 0.2981 J/g, respectively, indicating the

physisorption nature of the adsorption process due to low surface area of ACPK. The removal efficiency of Ni(II) ions by ACPK decreases as the temperature increases. The kinetic of the process was best described by pseudo-second order at different ACPK. The thermodynamic studies revealed that the ACPK-Ni(II) adsorption is exothermic and physical nature process.

ACKNOWLEDGMENTS

The authors would like to acknowledge the University of Sirte and chemistry department, Sebha University for providing us the required facilities to accomplish present research work.

REFERENCE

1. Hammaini, A., González, F., Ballester, A., Blázquez, M. & Munoz, J., 2007. Biosorption of Heavy Metals by Activated Sludge and Their Desorption Characteristics. Journal of environmental management, 84(4): 419-426. https://doi.org/10.1016/j.jenvman.2006.06.015
2. Krishna, R. H. & Swamy, A., 2012. Investigation on the Effect of Particle Size and Adsorption Kinetics to Removal of Hexavalent Chromium from the Aqueous Solutions Using Low Cost Sorbent. European Chemical Bulletin, 1(7): 258-262. http://dx.doi.org/10.17628/ecb.2012.1.258-262
3. Wang, J. & Guo, X., 2020. Adsorption Kinetic Models: Physical Meanings, Applications, and Solving Methods. Journal of Hazardous Materials, 390122156. https://doi.org/10.1016/j.jhazmat.2020.122156
4. Olayinka, K. O., Fatunsin, O. T. & Oyeyiola, A. O., 2009. Comparative Analysis of the Efficiencies of Two Low Cost Adsorbents in the Removal of Cr (Vi) and Ni (Ii) from Aqueous Solution. African Journal of Environmental Science and Technology, 3(11): https://doi.org/10.5897/AJEST09.087
5. Verla, A., Horsfall(Jnr), M. & Verla, E., 2012. Preparation and Characterization of Activated Carbon from Fluted Pumpkin (Telfairia Occidentalis Hook. F) Seed Shell. Asian journal of natural and applied sciences, 1(3): 39-50.
6. Patil, A. & Shrivastava, V., 2010. Adsorption of Ni (Ii) from Aqueous Solution on Delonix Regia (Gulmohar) Tree Bark. Archives of Applied Science Research, 2(2): 404-413.
7. Evbuomwan, B., Agbede, A. & Atuka, M., 2013. A Comparative Study of the Physico-Chemical Properties of Activated Carbon from Oil Palm Waste (Kernel Shell and Fibre). International Journal of Science and Engineering Investigations, 2(19): 75-79.
8. Nagy, B., Maicaneanu, A., Indolean, C., Burca, S., Silaghi-Dumitrescu, L. & Majdik, C., 2013. Cadmium (Ii) Ions Removal from Aqueous Solutions Using Romanian Untreated Fir Tree Sawdust–a Green Biosorbent. Acta Chimica Slovenica, 60(2): 263-273.
9. Singanan, M. & Peters, E., 2013. Removal of Toxic Heavy Metals from Synthetic Wastewater Using a Novel Biocarbon Technology. Journal of Environmental Chemical Engineering, 1(4): 884-890. https://doi.org/10.1016/j.jece.2013.07.030
10. Chakrapani, C., Babu, C., Vani, K. & Rao, K. S., 2010. Adsorption Kinetics for the Removal of Fluoride from Aqueous Solution by Activated Carbon Adsorbents Derived from the Peels of Selected Citrus Fruits. Journal of Chemistry, 7(S1): S419-S427. https://doi.org/10.1155/2010/582150
11. Pradhan, B. K. & Sandle, N., 1999. Effect of Different Oxidizing Agent Treatments on the Surface Properties of Activated Carbons. Carbon, 37(8): 1323-1332. https://doi.org/10.1016/S0008-6223(98)00328-5
12. Shahmohammadi-Kalalagh, S., Babazadeh, H., Nazemi, A. H. & Manshouri, M., 2011. Isotherm and Kinetic Studies on Adsorption of Pb, Zn and Cu by Kaolinite. Caspian Journal of Environmental Sciences, 9(2): 243-255.
13. Erhayem, M. & Sohn, M., 2014. Stability Studies for Titanium Dioxide Nanoparticles Upon Adsorption of Suwannee River Humic and Fulvic Acids and Natural Organic Matter. Science of the total environment, 468249-257. https://doi.org/10.1016/j.scitotenv.2013.08.038
14. Erhayem, M. & Sohn, M., 2014. Effect of Humic Acid Source on Humic Acid Adsorption onto Titanium Dioxide Nanoparticles. Science of the Total Environment, 47092-98. https://doi.org/10.1016/j.scitotenv.2013.09.063
15. Al-Anber, Z. A. & Al-Anber, M. A., 2008. Thermodynamics and Kinetic Studies of Iron (Iii) Adsorption by Olive Cake in a Batch System. Journal of the Mexican chemical society, 52 (2): 108-115. https://doi.org/10.29356/jmcs.v52i2.1055
16. Shelke, R., Madje, B., Bharad, J. & Ubale, M., 2009. Adsorption of Nickel (Ii), Copper (Ii) and Iron (Iii) from Aqueous Solution Using Ashoka Leaf Powder. International Journal of ChemTech Research, 1(4): 1318-1325.
17. Tseng, R.-L. & Wu, F.-C., 2008. Inferring the Favorable Adsorption Level and the Concurrent Multi-Stage Process with the Freundlich Constant. Journal of Hazardous Materials, 155(1-2): 277-287. https://doi.org/10.1016/j.jhazmat.2007.11.061
18. Salarirad, M. M. & Behnamfard, A., 2011. Modeling of Equilibrium Data for Free Cyanide Adsorption onto Activated Carbon by Linear and Non-Linear Regression Methods. in International Conference on Environment and Industrial Innovation, pp: 79-84.
19. Depci, T., Kul, A. R. & Önal, Y., 2012. Competitive Adsorption of Lead and Zinc from Aqueous Solution on Activated Carbon Prepared from Van Apple Pulp: Study in Single-and Multi-Solute Systems. Chemical engineering journal, 200224-236. https://doi.org/10.1016/j.cej.2012.06.077
20. Erdem, E., Karapinar, N. & Donat, R., 2004. The Removal of Heavy Metal Cations by Natural Zeolites. Journal of colloid and interface science, 280(2): 309-314. https://doi.org/10.1016/j.jcis.2004.08.028
21. Ho, Y., Porter, J. & McKay, G., 2002. Equilibrium Isotherm Studies for the Sorption of Divalent Metal Ions onto Peat: Copper, Nickel and Lead Single Component Systems. Water, Air, & Soil Pollution, 141(1): 1-33. https://doi.org/10.1023/A:1021304828010
22. Das, B., Mondal, N. K., Roy, P. & Chattaraj, S., 2013. Equilibrium, Kinetic and Thermodynamic Study on Chromium (Vi) Removal from Aqueous Solution Using Pistia Stratiotes Biomass. Chemical Science Transactions, 2(1): 85-104. https://doi.org/10.7598/cst2013.318
23. Atar, N., Olgun, A. & Wang, S., 2012. Adsorption of Cadmium (Ii) and Zinc (Ii) on Boron Enrichment Process Waste in Aqueous Solutions: Batch and Fixed-Bed System Studies. Chemical Engineering Journal, 1921-7. https://doi.org/10.1016/j.cej.2012.03.067

Persian Abstract

DOI: 10.5829/ijee.2020.11.04.12

چکیده

هسته نخل (PK) با فعال سازی شیمیایی (HNO_3 در ۲۳۰ درجه سانتیگراد) فعال شد تا یون های Ni (II) از محلول های آبی حذف شود. خواص فیزیکوشیمیایی PK گزارش شده است. تجزیه و تحلیل FT-IR تغییر در تعداد موج و میزان جذب را نشان می دهد Ni(II) جذب بر روی سطح کربن-PK فعال است. برای تعیین محتوای فلزات در کربن فعال-PK از روش فلورسانس اشعه ایکس پراکندگی انرژی استفاده شد و نشان داد که فلزات موجود در کربن فعال-PK در کاربردهای توصیه شده انسانی است. حداکثر حذف یون های Ni(II) قرار بود ۴۹/۷ درصد در pH 4.6باشد و تعادل در ۸۰ دقیقه برسد. بازده حذف یونهای Ni(II) با افزایش دوز PK-activated افزایش یافته و مقدار بهینه دوز کربن-PK فعال ۷۰ میلی گرم یافت. pH مطلوب ۴.۶ بود. ایزوترم ، سینتیک و ترمودینامیک مورد مطالعه قرار گرفت. جذب – Ni(II) کربن-PK فعال برای پیروی از ایزوترم فروندلیچ بر اساس مقادیر ضریب همبستگی و جذب فیزیکی از میانگین انرژی آزاد یافت شده توسط Dubinin-Radushkevich ، که توسط داده های میکرو کالری متری ایزوترمال تأیید شده است ، پیدا شد. گرمای فرآیند جذب با استفاده از مدل Temkin Isotherm 1.58 کیلوژول بر مول است. داده های جنبشی جذب به ترتیب دوم با سرعت ثابت جنبشی در محدوده ۱.۸۲-۸۳.۵ گرم در گرم در دقیقه به خوبی توصیف شدند و توسط مدل انتشار درون ذره ای کنترل نشدند. مطالعات ترمودینامیکی نشان داد که فرآیند جذب Ni(II) -ACPK به دلیل مقادیر منفی Δ(9/30-J/mol) H گرمازا است و به دلیل مقادیر منفی Δ(9/14-J / mol) S فرآیند طبیعی است. بزرگی Ea 15.04 kJ/mol است، که جذب فیزیکی در طبیعت ثابت شده است.